



Automotive Sensors and Actuators, Laboratory

WINTER TERM 2017/2018

Yashas Nagaraj Udupa | Reg. No: 1647695 | February 15, 2018

Modeling of a Mechatronic System

Objectives

The objective of ABS is to manipulate the wheel slip so that a maximum friction is obtained and the steering stability (also known as the lateral stability) is maintained. That is, to make the vehicle stop in the shortest distance possible while maintaining the directional control. The purpose of implementation and Analysis of simple ABS system is to provide a general overview of this topic and to show the model-based design of a mechatronics vehicle dynamics system on the basis of a basic example.

The main objectives of this modelling are to attain the following:

- Derivation of the motion equations for a simple ABS system and modelling in Matlab/Simulink.
- Examination of the vehicle dynamics by means of simulation.
- Implementation of a simple control strategy.

Introduction

The theory behind anti-lock brakes is simple. A skidding wheel (where the tire contact patch is sliding relative to the road) has less traction than a non-skidding wheel. If the vehicle is being held on ice and if the wheels are spinning then it has no traction. This is because the contact patch is sliding relative to the ice. By keeping the wheels from skidding while the vehicle slows down, anti-lock brakes benefit in two ways: It tends to stop the vehicle faster, and it is possible to steer while the vehicle is in stage to stop. Good drivers have always pumped the brake pedal during panic stops to avoid wheel lock up and the loss of steering control. ABS simply get the pumping job done much faster and in much precise manner than the fastest human foot. Anti-lock Brake System (ABS) is the advanced system of brake in automobile and it was developed to base on the adhesion characteristic between the tire and the road. ABS can automatic amend wheel press to prevent wheel from locking at braking. ABS can improve braking efficiency, shortened braking distance, prevent wheel sideslip, decrease to braise tire.

1.1 Modeling

1.1.1 Motion Equations

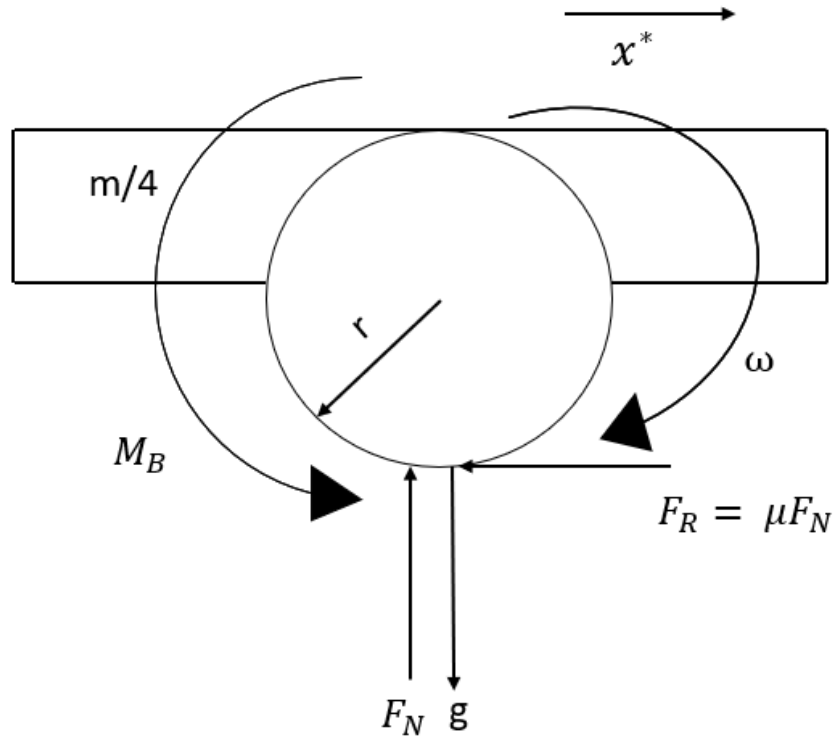


Fig 1: Diagram of a Kinetic chart of the wheel

$$\mathbf{F} = \mathbf{ma} \quad (\text{Linear Motion})$$

Based on Newton's 2nd law the equations of motion could be described as following

$$(\mathbf{m}/4 + m_{tire}) * \frac{dx^*}{dt} = -F_R \quad \dots\dots\dots (i)$$

$$\text{where } F_R = \mu F_N \quad \dots\dots\dots, \quad (ii)$$

$$\forall F_N = \frac{m}{4}g \quad \dots\dots\dots (iii)$$

m_{tire} = mass of tire

F_R = Frictional force

m = mass of a vehicle

F_N = Normal force

μ = Friction Coefficient

g = Gravitational constant = 9.8 m/s^2

The principle of ABS is based on the kinetics among tire, braking disc and ground. Considering all the exerting factors the analysis of a single wheel kinetics can be done as below. The kinetic equation is

Torque equation given by, $\tau = I\alpha$ (Rotation)

→ By equilibrium,

$$I \frac{d\omega}{dt} - F_R \cdot r_{\text{rad}} + M_B = 0$$

$$\Rightarrow I \frac{d\omega}{dt} = F_R \cdot r_{\text{rad}} - M_B \dots\dots\dots (iv)$$

$$\text{where } I = m_{\text{tire}} \cdot \left(\frac{r_i^2 + r_0^2}{2} \right)$$

$\frac{d\omega}{dt}$ = Angular acceleration

M_B = Braking Moment

F_N = Normal force

I = Moment of Inertia

1.1.2 Tire Model

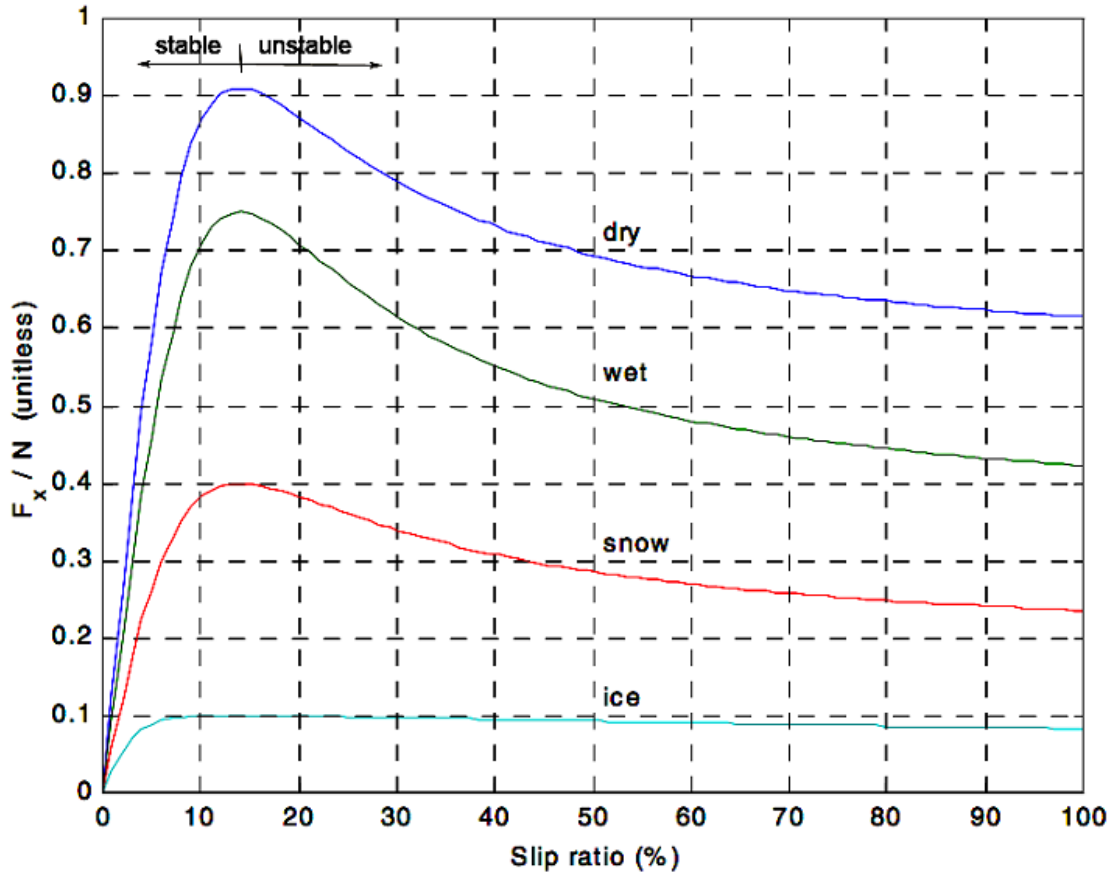


Fig 2: Typical tire longitudinal friction

1. Tires are the hard-working key element of ABS controls. Tire models express tire forces as a function of tire longitudinal and lateral slips, tire normal force, and surface conditions. The tire longitudinal slip is defined by the difference between a true absolute vehicle speed, equivalent to a free rotating wheel speed, and an actual measured wheel speed after being normalized by the same vehicle speed. Unfortunately, the absolute vehicle speed cannot be measured easily. The normal force has direct effect on wheel dynamics, but cannot be measured at a low cost. Also, it is rather safe to say that the surface condition is unknown in real time. Fig. 2 shows typical longitudinal Friction curves as a function of a wheel slip on several surface conditions for cases without a wheel side slip.

The longitudinal slip of wheel is defined as

$$S = \frac{V_{car} - V_w}{V_{car}}$$

$$\text{i.e, } S = \frac{V_{car} - \omega r}{V_{car}}$$

As the figure shows, there is a wide variation of peak slip points and peak friction (μ) values depending upon surface types.

Where ω , R , and V denote the wheel angular velocity, the wheel rolling radius, and the vehicle forward velocity, respectively. In normal driving conditions, $V = \omega R$, therefore $S = 0$.

In severe braking, it is common to have $\omega = 0$ while $S = 1$, which is called wheel lockup. Wheel lockup is undesirable since it prolongs the stopping distance and causes the loss of direction control. Empirically when wheel is freewheeling, Wheel Slip gives rise to 0% and 100% when wheel is fully locked. Maximum braking forces occur when wheel slip is in the range of 10% to 30%. So, the optimal value lies within this range where it does a reasonable job in controlling the vehicle dynamics in order not to lose its stability and provides an optimal deceleration to stop the vehicle at the considerable amount of time. And a side force or a slip angle plays an important in controlling the vehicle dynamics when selecting the nominal slip while the ABS is activated during cornering.

The relation of the frictional coefficient μ versus wheel slip ratio S , provides the explanation of the ability of the ABS to maintain vehicle steerability and stability, and still produce shorter stopping distances than those of locked wheel stop. The friction coefficient can vary in a very wide range, depending on factors like:

- (a) Road surface conditions (dry or wet),
- (b) Tire side - slip angle,
- (c) Tire brand (summer tire, winter tire),
- (d) Vehicle speed, and
- (e) The slip ratio between the tire and the road.

$$\mu(s) = c_1 \cdot (1 - e^{-c_2 s}) - c_3 s$$

Where C_1 is the maximum value of friction curve;

C_2 the friction curve shapes;

C_3 the friction curve difference between the maximum value and the value at $S = 1$;

2. By trial and error method the appropriate values of C_1 , C_2 and C_3 is determined and the values that are used to simulate the Bukhart's model function is as shown below and the simulated behaviour of friction coefficient μ as a function of the slip value for different road surfaces i.e dry asphalt and snow lane is as shown in fig3 and fig4 respectively.

For Dry asphalt:

$$C_1 = 0.957, C_2 = 33.922, C_3 = 0.347.$$

For Snow lane:

$$C_1 = 0.43, C_2 = 30, C_3 = 0.15.$$

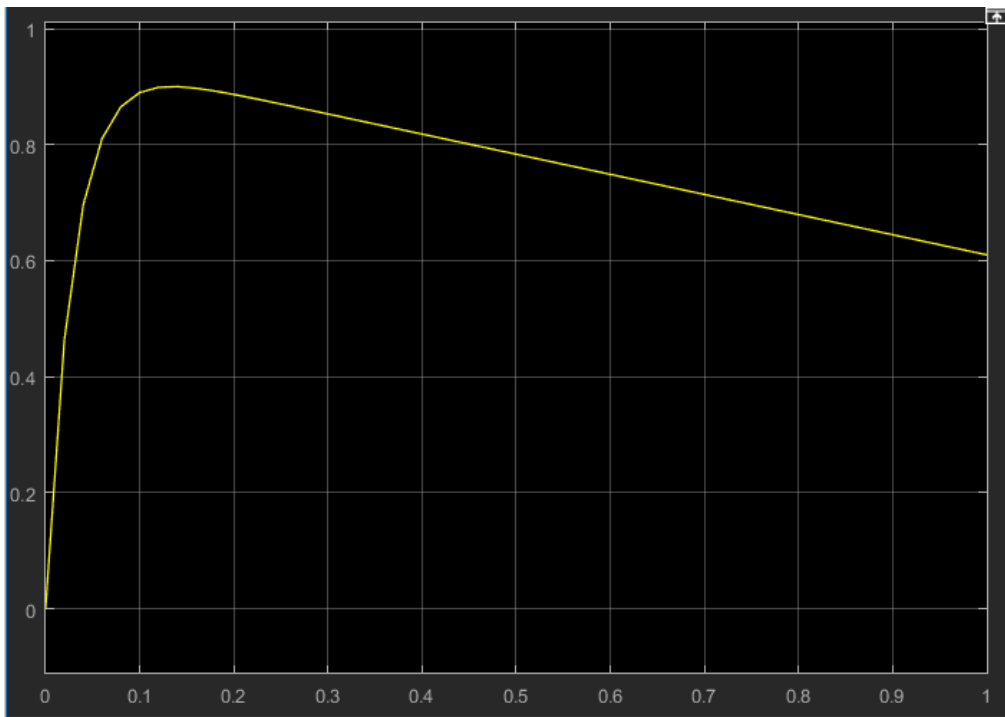


Fig 3: Dry asphalt

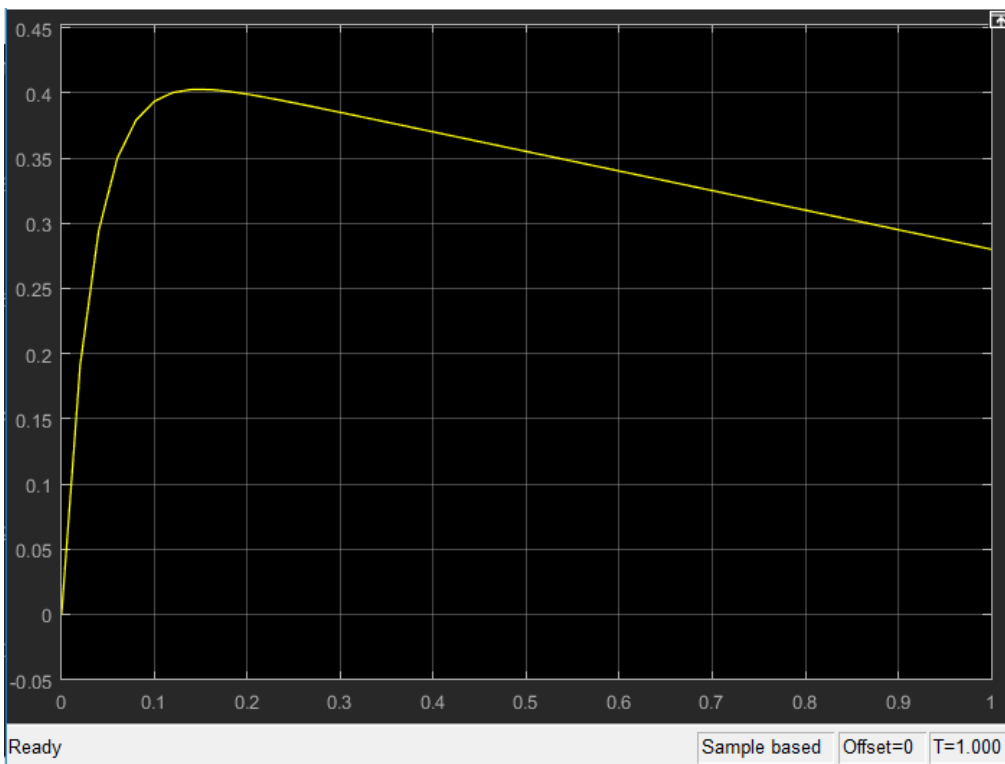


Fig 4: Snow lane

1.1.3 Brake Model

1. The minimum braking torque at which the wheel safely blocks is determined by the following deductions i.e,

$$M_{Bmin} = F_{Beff} * r$$

$$M_{Bmin} = \mu * F_N * r$$

Braking force is equal to the product of the coefficient of friction between the tyre and the ground and normal reaction on wheel.

$$M_{Bmin} = \mu * (m/4 + m_{tire}) * g * r \quad (\text{From Eq iv})$$

Coefficient of friction(Optimal) to attain the effective braking force is the value at which the maximum braking force is applied.

And it changes for change in surface conditions i.e,

- i)For dry surface, $\mu = 0.9$
- i)For wet surface, $\mu = 0.75$
- i)For Snow surface, $\mu = 0.4$
- i)For ice surface, $\mu = 0.1$

$$\rightarrow M_{Bmin} = 0.9 * \left(\frac{9.9}{4} + 0.28\right) * 9.8 * 0.06 \quad (\text{Assuming for dry surface})$$

$$\rightarrow M_{Bmin} = 1.457946 \text{ Nm}$$

F_{Beff} = Braking force between tire and road surface

r = Effective rolling radius of tire

μ = Co-efficient of friction between tire and road surface

g = Acceleration due to gravity = 9.8 m/s^2

1.2 Implementation of a Model on the PC

1.2.1 Simulation

Simulation results of full braking scenario with varying ground conditions as per the given boundary conditions i.e, $V_0 = 10 \text{ m/s}$ and to stop the simulation once when the vehicle is at verge to stop.

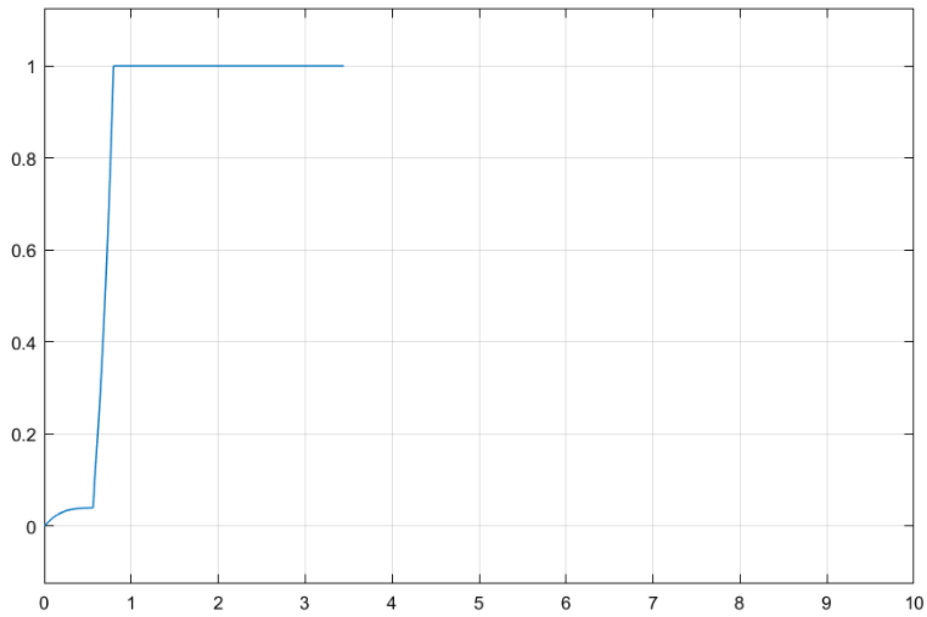


Fig 5: Slip without ABS

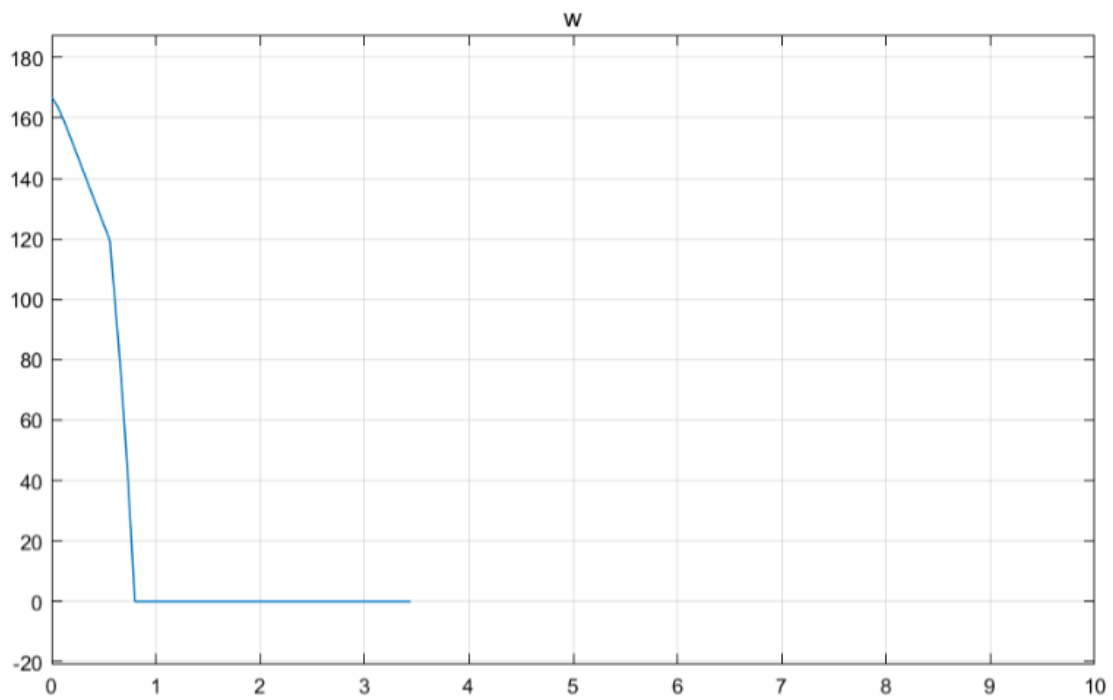


Fig 6: Angular velocity without ABS

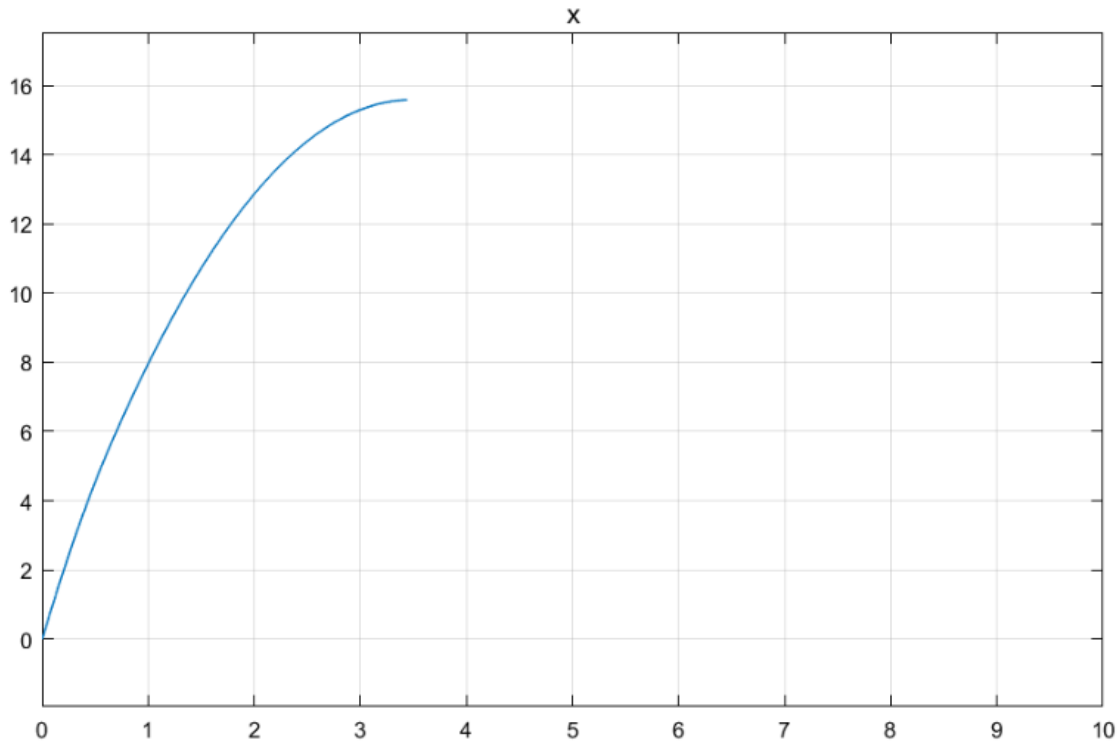


Fig 7: Stopping Distance without ABS

1.4 Design of a Controller

1. A feedback control system is a closed loop control system in which a sensor monitors the output (slip ratio) and feeds data to the controller which adjusts the control (brake pressure modulator) as necessary to maintain the desired system output (match the wheel slip ratio to the reference value of slip ratio).

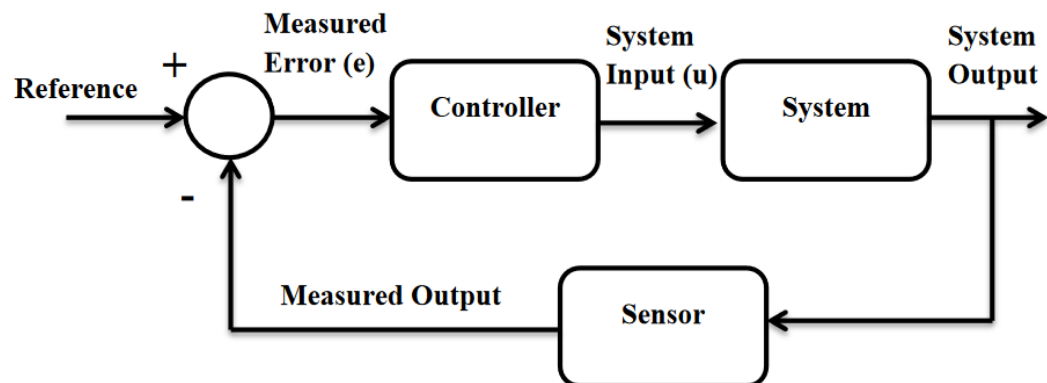


Fig 8: Block Diagram of Feedback Control System

Fig 8 shows the block diagram of feedback control system

2. Simulation results of implementation of Simple Relay Controller. Relatively it has an improvement in terms of Stopping Distance i.e as per simulation results at quite a lesser distance the vehicle is tend to be stopping when it is controlled by relay controller.

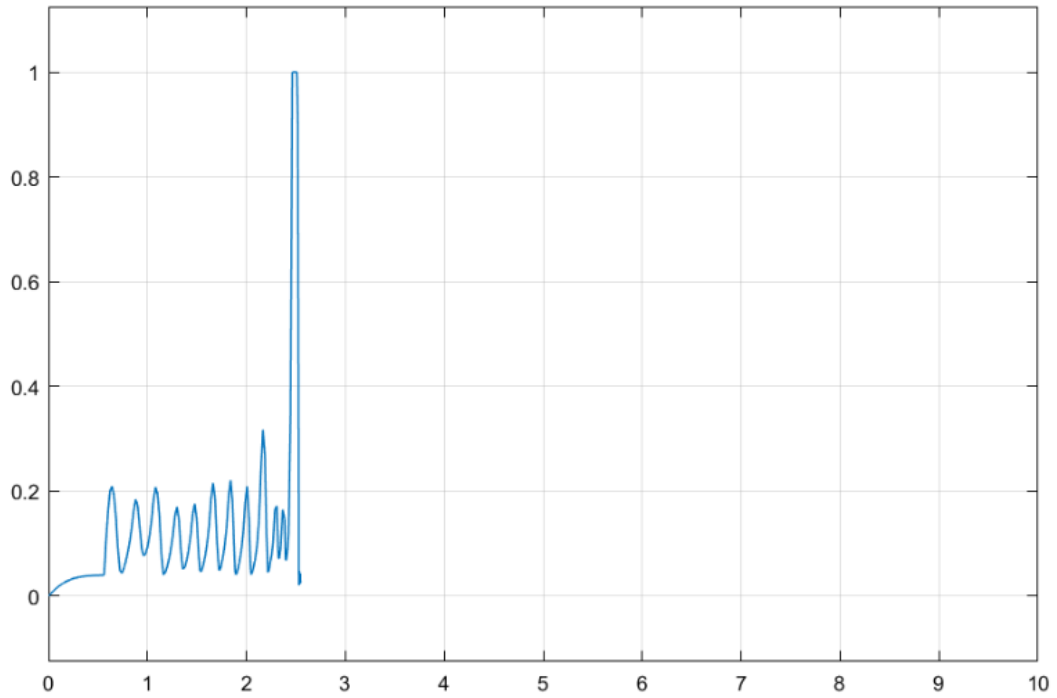


Fig 9: Slip with ABS

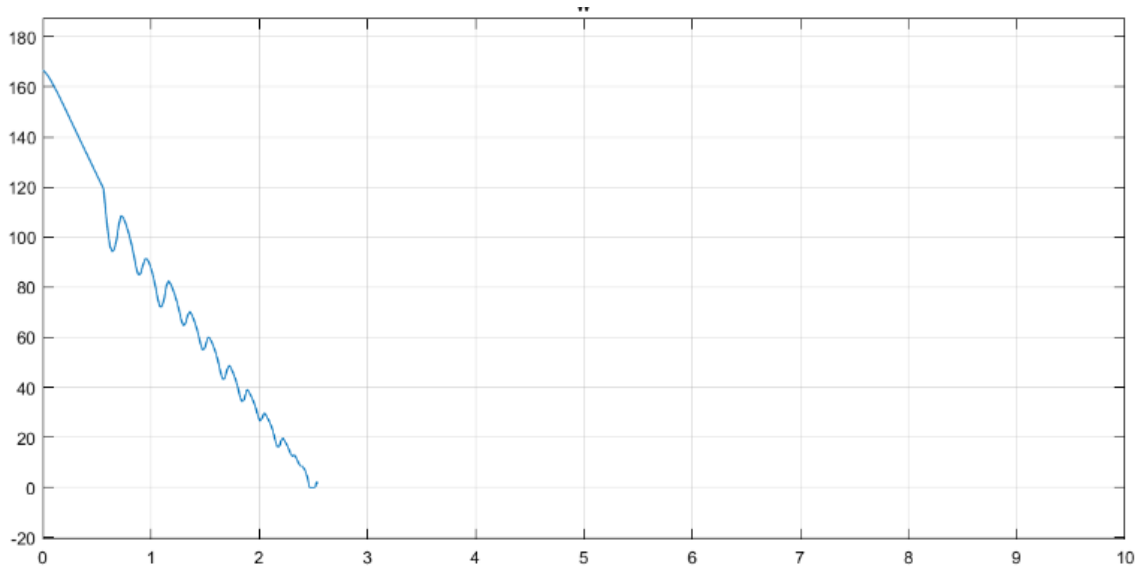


Fig 10: Angular velocity with ABS

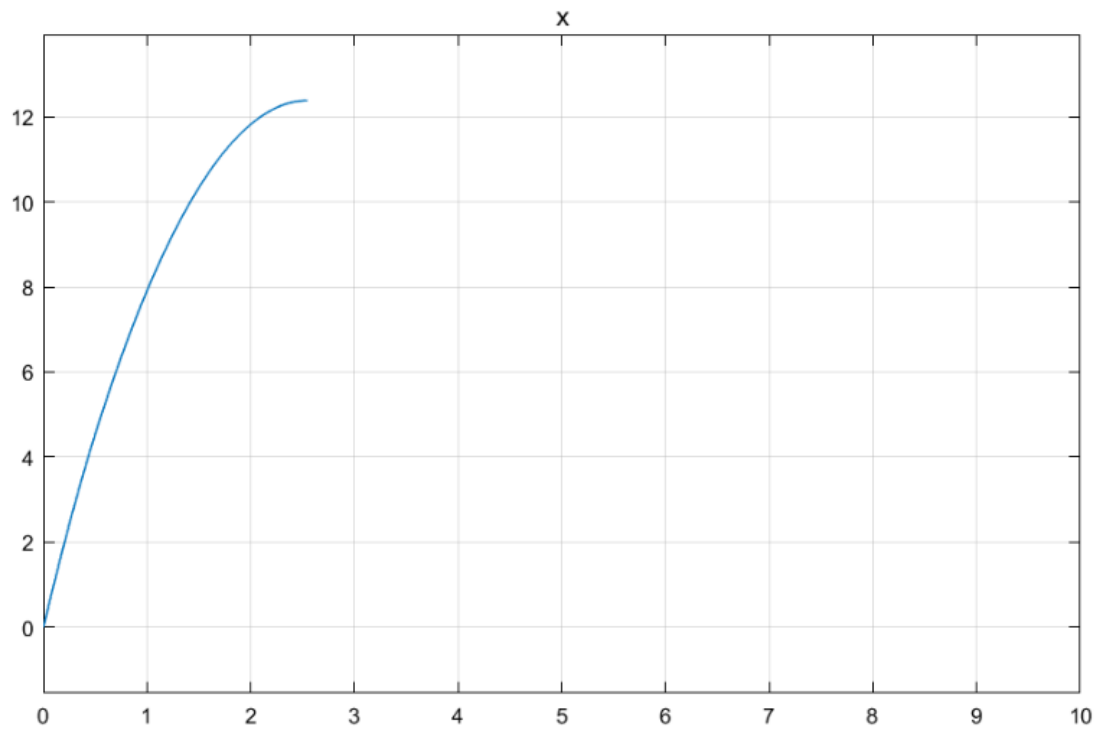


Fig 11: Stopping Distance with ABS

Sensor Data Fusion for Velocity Estimation

Objectives

The objective of this exercise is to determine the Vehicle speed using the rotational speed of vehicle wheels which are estimated using Wheel speed sensors and to Familiarize with the development environment by writing a simple test program following to which the functionality of the implementation is being checked using a function generator (Tectronix AWG).

The main tasks of this module are to achieve the following:

- Modeling of the sensor system in Matlab.
- Fusion of acceleration measurement and speed measurement using the Kalman filter.
- Filter Implementation of the speed measurement at the test vehicle (C programming language).
- Test drives and measurements for concept evaluation.

Introduction

The main motivation for determining the vehicle speed by means of wheel speed sensors along with other physical quantities such as acceleration, position etc fused is to obtain improved decision making and reliability in accuracy of the estimated Velocity values. Resulting in improved overall system performance. The Kalman Filter (KF) is one of the most widely used methods for tracking and estimation due to its optimality, tractability and robustness. KF is a recursive predicted filter based on state techniques and recurrent algorithms. In fact, this filter is the collection of mathematical equations to estimate effective state for a dynamic system. The performance of dynamic system can disrupt with some white noises.

2.1 Wheel Speed and Vehicle Speed

2.1.1 Demonstrator implementation

1. In order to select the suitable pre-scaler factor, the feasible N value to be chosen wherein to do that the N value is to be found out for both the speed values i.e for 0.1 m/s and 60 km/h.

And N value is given by

$$N = \frac{T_b \times \text{freq}}{65535} \dots\dots\dots (i)$$

Where T_b is the time duration between consecutive pulses.

As per the data, the rotating disc features 12 slots and radius of a disc is 0.06m, the T_b value can deduced as follows,

$$T_b = \frac{T}{12}$$

$$\text{Where } T = \frac{2\pi}{\omega}$$

$$\rightarrow T_b = \frac{\frac{2\pi}{\omega}}{12} \quad (\text{Note : } \omega = \frac{V}{R})$$

$$\rightarrow T_b = \frac{\pi \times R}{6 \times V}$$

$$T_b = \frac{3.1415 \times 0.06}{6 \times 0.1} \quad (\text{Consider for velocity 0.1m/s})$$

$$T_b = 0.31415 \text{ s}$$

Similarly for velocity 60 kmph

$$T_b = 0.3133 \text{ ms}$$

Considering these two for values for computing N using (i) , a suitable prescaler factor which could be applicable for both minimum and maximum speed turned out to be a factor 56 and the nearest prescaler is to have chosen 64.

2. In order to interpret the behaviour of a wheel speed, those signals are simulated using signal generator where appropriate frequency signal is being obtained. And this signal is being fed into Input Capture register of the Microcontroller (ICR1). Whenever there is a voltage in the signal it is being

interrogated by the Interrupt service routine which captures the exact value of a counter during an event (Rising edge). And for the necessary environment setup i.e to choose to appropriate pre-scalar value and to enable the timer interrupt.

The values that are set for TCCR1A, TCCR1B and TIMSK1 are 0x00, 0x43 and 0x21 correspondingly. And the firmware is being implemented handling the in between interrupts that occur within a consecutive pulse by appending those counter overflow values to the initial release counter value and final ending counter value. And then using this counter value the wheel speed is being calculated which is then communicated byte wise over a CAN bus to analyse in the Canoe window. And it is as shown in the below figures.

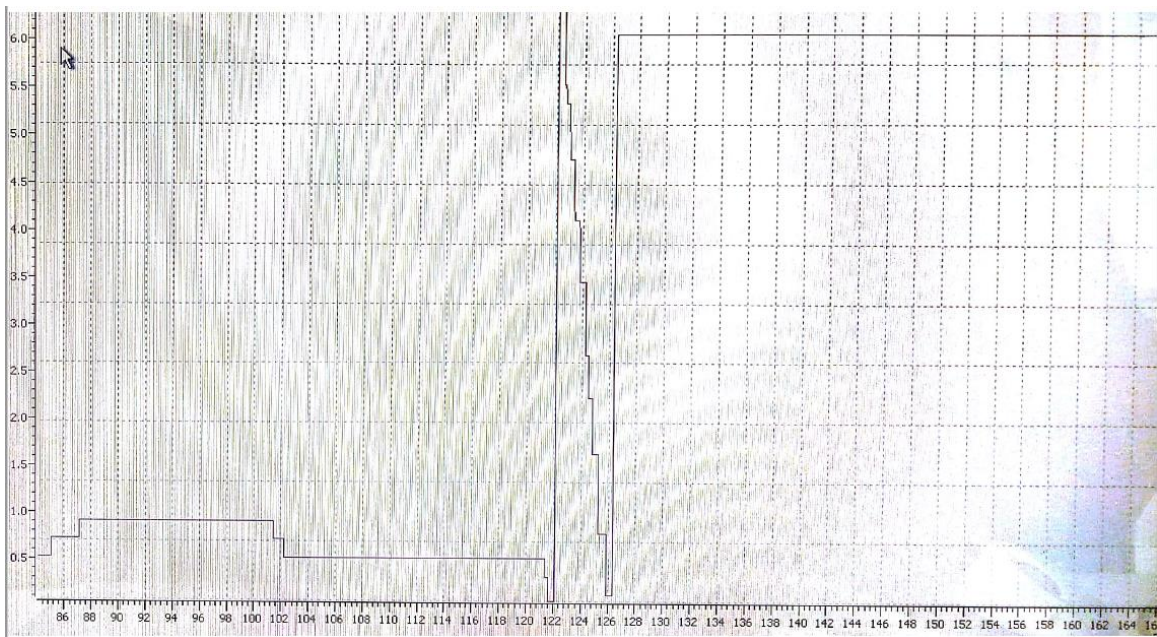


Figure 1: Wheel speed analysis - CANOE window.

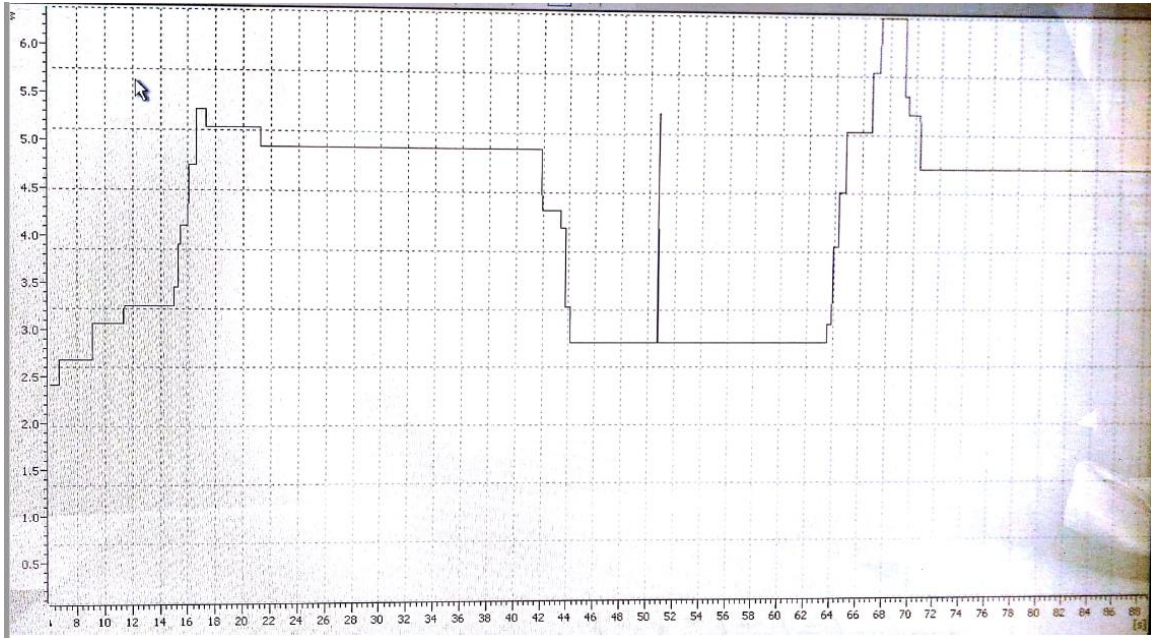


Figure 2: Wheel speed analysis - CANOE window.

2.3.3 Kalman Filter

1. Kalman filter is an optimal data fusion algorithm under certain assumptions. Kalman filter incorporates all available information i.e.,

- Knowledge of the system and measurement device dynamics.
- Statistical description of the system noises, measurement errors, and uncertainty in the dynamics models.
- Any available information about initial conditions of the variables of interest.

Kalman filter in our case can be used as a mechanism that estimates a process by using a form of feedback control: the filter estimates the process state at some time and then obtains feedback in the form of (noisy) measurements. As such, the equations for the Kalman filter fall into two groups: time update equations and measurement update equations. The time update equations are responsible for projecting forward (in time) the current state and error covariance estimates to obtain the a priori estimates for the next time step. The measurement update equations are responsible for the feedback—i.e. for incorporating a new measurement into the a priori estimate to obtain an improved a posteriori estimate.

The time update equations can also be thought of as predictor equations, while the measurement update equations can be thought of as corrector equations. Indeed, the final

estimation algorithm resembles that of a predictor-corrector algorithm for solving numerical problems as shown below in Figure 1

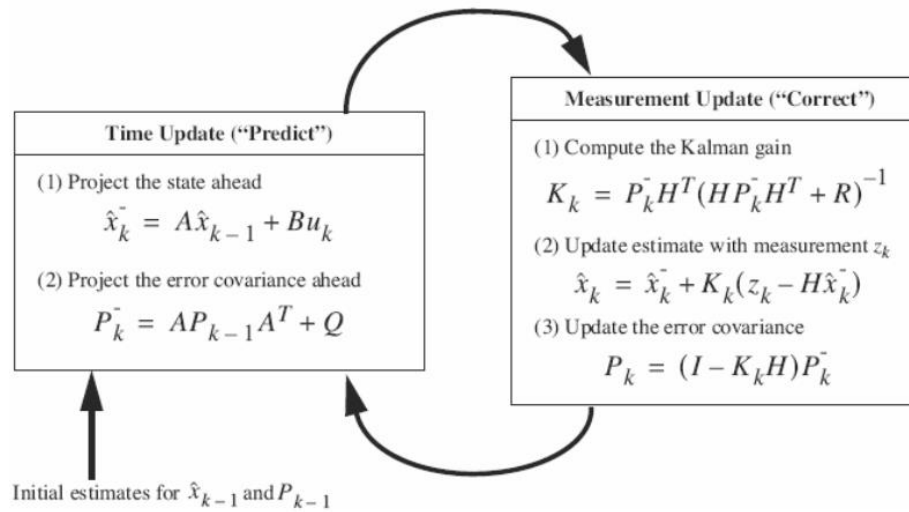


Figure 1.

The above is the Kalman filter cycle. The time update projects the current state estimate ahead in time. The measurement update adjusts the projected estimate by an actual measurement at that time.

The Kalman Gain (K in measurement update equation 1) is derived from minimizing a posteriori error covariance. What the Kalman Gain tells us is that as the measurement error covariance R approaches zero, the actual measurement z is "trusted" more and more, while the predicted measurement Hx (here x is estimated value of x) is trusted less and less.

On the other hand, as the a priori estimate error covariance P approaches zero the actual measurement is trusted less and less, while the predicted measurement is trusted more and more.

A typical application example of finding out the position of a moving vehicle was considered to describe the Kalman filter principles. In, where just by trusting the readings from say an instance with GPS to find out the position of a vehicle is strongly not encouraged as it's prone to external factors which can deplete the accuracy of position measurement(noise). Henceforth, along with the values of GPS, the other values coming in may be from acceleration sensor or wheel speed sensor is combined together to get an improved position reading in the presence of process and measurement noise. The main idea behind the sensor fusion is as said to improve the accuracy of the measurement.

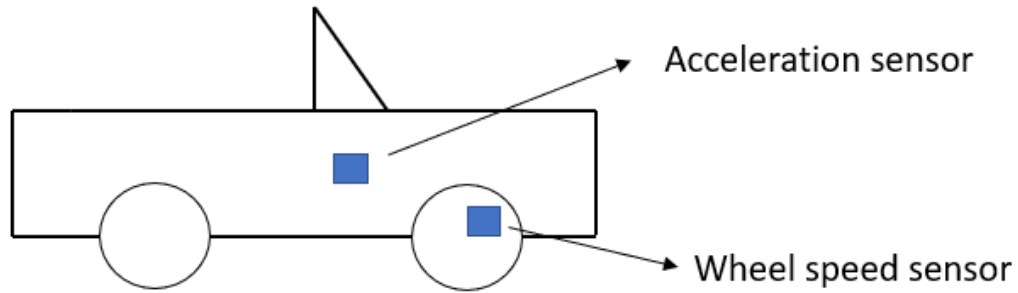


Figure 2.

And the measurements are basically the probability density functions, combining the measurement values are nothing but product of multiple Normal distribution functions. Resultant to which another fine-tuned Gaussian distribution function.

The initial state of the system (at time $t = 0$ s) is known to a reasonable accuracy, as shown in Figure 3. The location of the vehicle is given by a Gaussian pdf. At the next time instance

($t = 1$ s), we can estimate the new position of the vehicle, based on known limitations such as its position and velocity at $t = 0$, its maximum possible acceleration and deceleration, etc. In

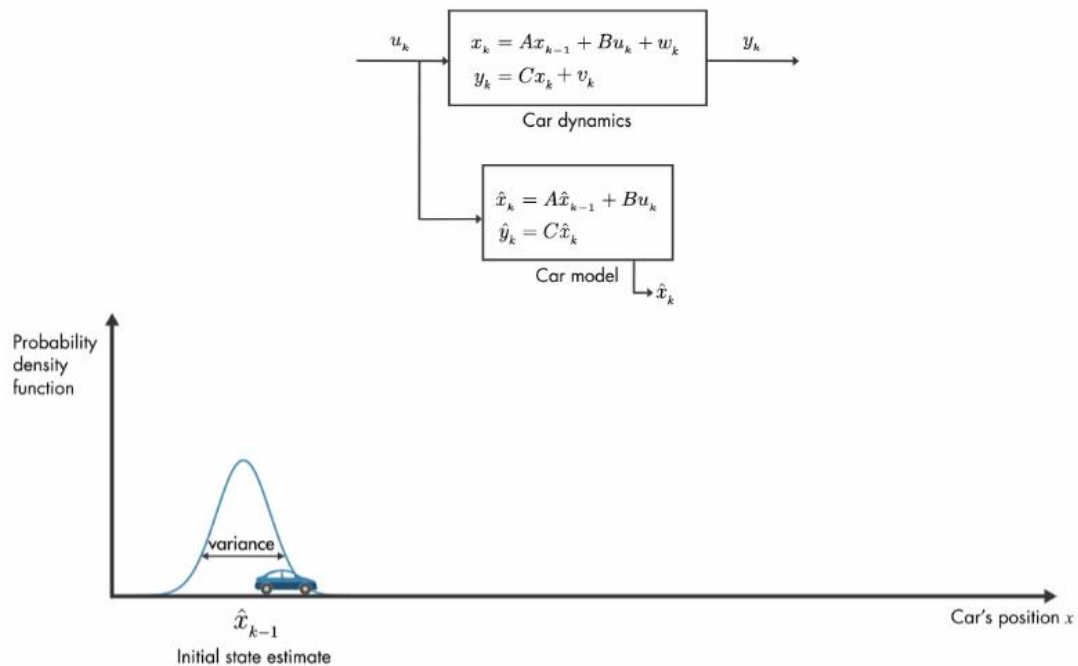


Figure 3.

practice, we may have some knowledge of the control inputs on the brake or accelerator by the driver. In any case, we have a prediction of the new position of the vehicle, represented

in Figure 4 by a new Gaussian pdf with a new mean and variance.

The variance has increased, representing our reduced certainty in the accuracy of our position estimate compared to $t=0$, due to the uncertainty associated with any process noise from accelerations or decelerations undertaken from time $t=0$ to time $t=1$.

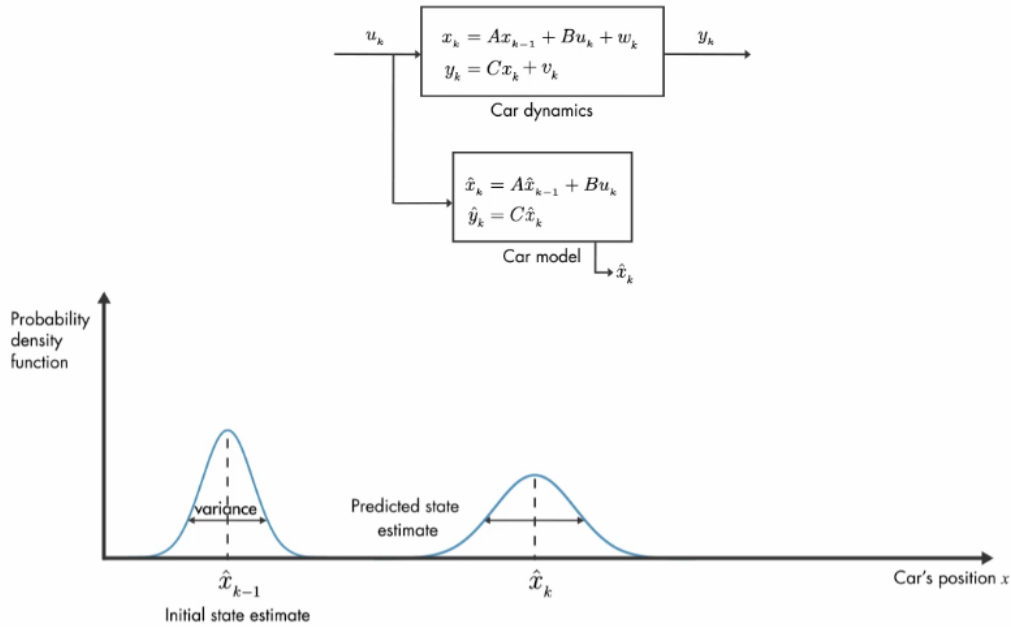


Figure 4.

At $t=1$, we also make a measurement of the location of the vehicle using the radio positioning system, and this is represented by the orange Gaussian pdf in Figure 5.

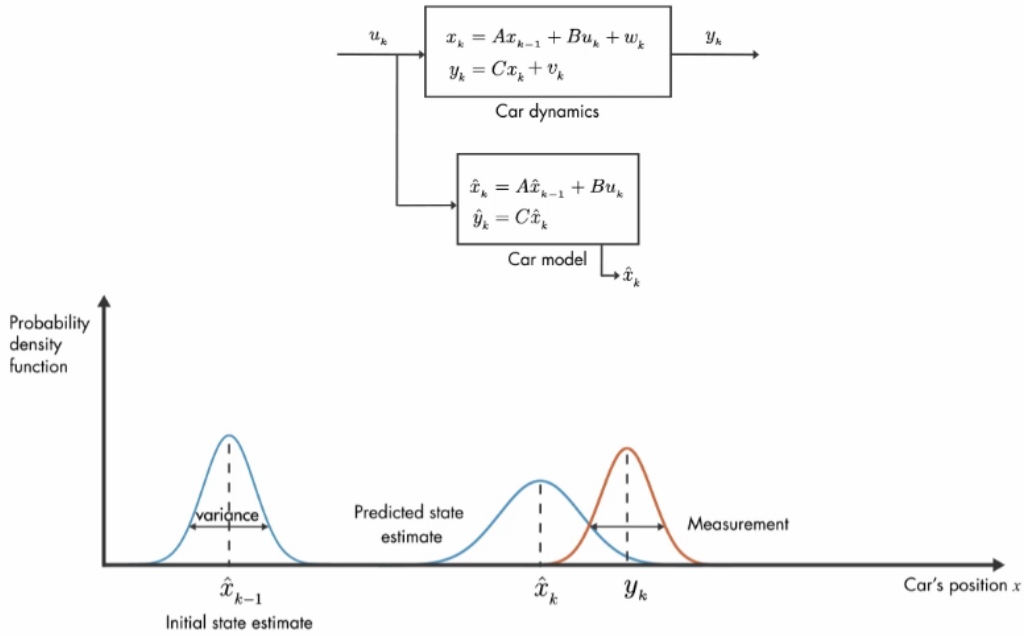


Figure 5.

The best estimate we can make of the location of the vehicle is provided by combining our knowledge from the prediction and the measurement. This is achieved by multiplying the two corresponding pdfs together. This is represented by the grey pdf in Figure 6. A key property of the Gaussian function is exploited at this point: the product of two Gaussian functions is another Gaussian function. This is critical as it permits an endless number of Gaussian pdfs to be multiplied over time, but the resulting function does not increase in complexity or number of terms; after each time epoch the new pdf is fully represented by a Gaussian function. This is the key to the elegant recursive properties of the Kalman filter.

The stages described above in the figures are now considered again mathematically to derive the Kalman filter measurement update equations. The prediction pdf represented by a little large variance Gaussian function in Figure 4 is given by the equation

$$y_1(r; \mu_1, \sigma_1) \triangleq \frac{1}{\sqrt{2\pi\sigma_1^2}} e^{-\frac{(r-\mu_1)^2}{2\sigma_1^2}}.$$

The measurement pdf represented by the Gaussian function in Figure 5 is given by

$$y_2(r; \mu_2, \sigma_2) \triangleq \frac{1}{\sqrt{2\pi\sigma_2^2}} e^{-\frac{(r-\mu_2)^2}{2\sigma_2^2}}$$

The information provided by these two pdfs is fused by multiplying the two together, i.e., considering the prediction and the measurement together (see Figure 6). The new pdf representing the fusion of the information from the prediction and measurement, and our best current estimate of the system, is therefore given by the product of these two Gaussian functions

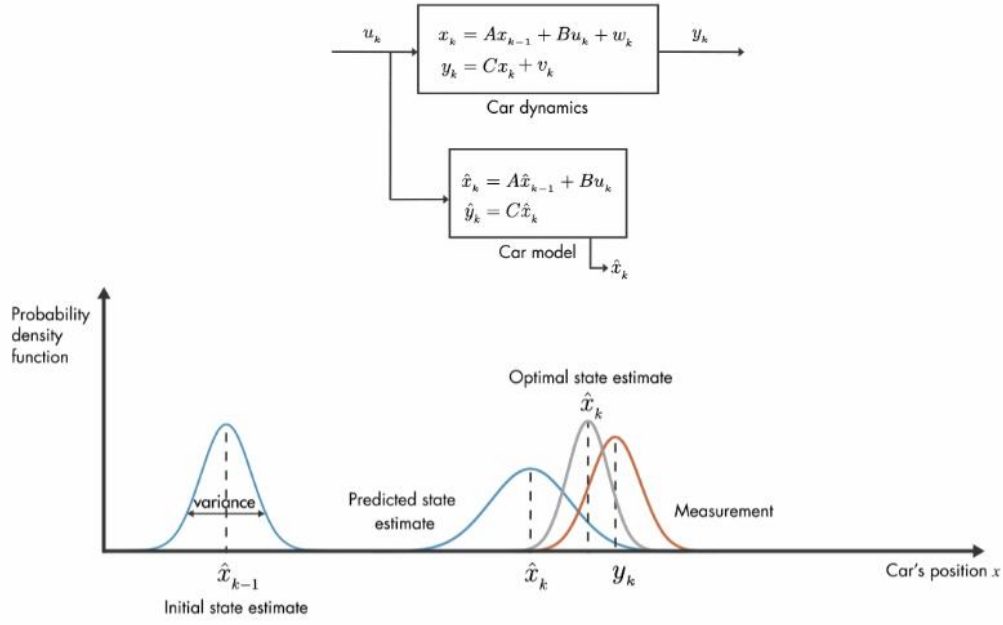


Figure 6.

$$\begin{aligned}
 & y_{\text{fused}}(r; \mu_1, \sigma_1, \mu_2, \sigma_2) \\
 &= \frac{1}{\sqrt{2\pi\sigma_1^2}} e^{-\frac{(r-\mu_1)^2}{2\sigma_1^2}} \times \frac{1}{\sqrt{2\pi\sigma_2^2}} e^{-\frac{(r-\mu_2)^2}{2\sigma_2^2}} \\
 &= \frac{1}{2\pi\sqrt{\sigma_1^2\sigma_2^2}} e^{-\left(\frac{(r-\mu_1)^2}{2\sigma_1^2} + \frac{(r-\mu_2)^2}{2\sigma_2^2}\right)}.
 \end{aligned}$$

The quadratic terms in this new function can be expanded and then the whole expression rewritten in Gaussian form

$$\begin{aligned}
 & y_{\text{fused}}(r; \mu_{\text{fused}}, \sigma_{\text{fused}}) \\
 &= \frac{1}{\sqrt{2\pi\sigma_{\text{fused}}^2}} e^{-\frac{(r-\mu_{\text{fused}})^2}{2\sigma_{\text{fused}}^2}},
 \end{aligned}$$

where

$$\begin{aligned}
 \mu_{\text{fused}} &= \frac{\mu_1\sigma_2^2 + \mu_2\sigma_1^2}{\sigma_1^2 + \sigma_2^2} \\
 &= \mu_1 + \frac{\sigma_1^2(\mu_2 - \mu_1)}{\sigma_1^2 + \sigma_2^2}
 \end{aligned}$$

and

$$\sigma_{\text{fused}}^2 = \frac{\sigma_1^2\sigma_2^2}{\sigma_1^2 + \sigma_2^2} = \sigma_1^2 - \frac{\sigma_1^4}{\sigma_1^2 + \sigma_2^2}.$$

These last two equations represent the measurement update steps of the Kalman filter algorithm, as will be shown explicitly below. However, to present a more general case, we need to consider an extension to this example.

2. The above theory is being tried to be simulated in MATLAB model. Accordingly, the necessary assumptions are made before fusing the sensor readings. Here, we are trying to estimate the position of a vehicle by considering values from three sensor system. Those are position, velocity and acceleration. Therefore, following are the assumptions that are made in terms of the state transition matrix i.e.,

$$\begin{aligned} X_t &= X_{t-1} + (X_{t-1}^* * \Delta t) + \frac{f * (\Delta t) * (\Delta t)}{2m} \\ X_t^* &= X_{t-1}^* + \frac{f * \Delta t}{m} \\ X_t^{**} &= X_{t-1}^{**} \end{aligned}$$

These linear equations can be written in matrix form as

$$F = \begin{bmatrix} 1 & Ts & 0.5*Ts^2; & 0 & 1 & Ts; & 0 & 0 & 1 \end{bmatrix};$$

3. The process noise covariance (Q) and measurement noise covariance (R) is assumed as follows:

$$Q = \begin{bmatrix} 2 & 0 & 0; & 0 & 1 & 0; & 0 & 0 & EPSQ \end{bmatrix};$$

$$R = \begin{bmatrix} 0.1 & 0; & 0 & 0.1 \end{bmatrix};$$

4. When the above assumptions are plugged into the provided MATLAB file, below is the plot that is obtained which informs about the accuracy of the readings.

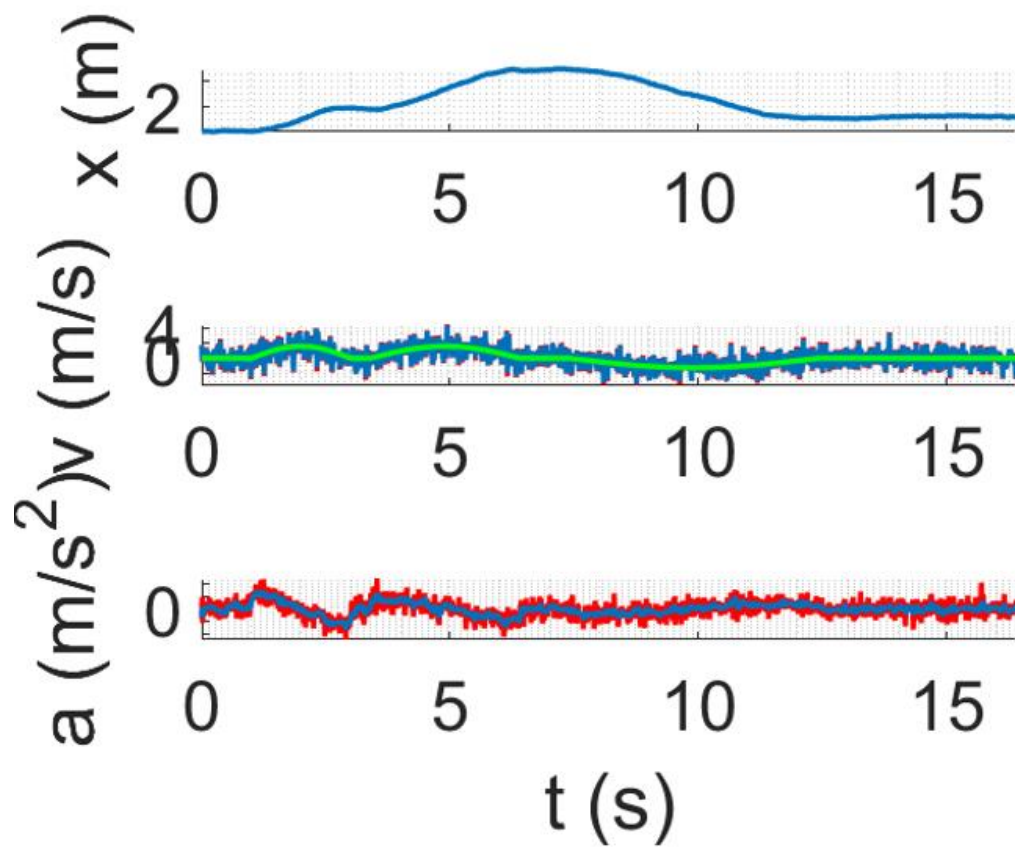


Figure 7.

Implementation and Analysis of an FMCW Radar System

Objectives

The objective of this exercise is to determine the speed and distance to objects in the environment by means of FMCW radar systems. For speed measurement, the radar is operated in the continuous wave mode and a frequency shift is evaluated according to the Doppler effect. For distance measurement, the continuous-wave signal is modulated in its frequency and a run-time measurement is performed. For this purpose, the beat frequency between the transmitted and the received signal is determined

The main tasks of this module are to achieve the following:

- Distance and speed measurement using FMCW radar (components, setup, algorithms).
- Analysis of Lab demonstrator (controls, signals, matching).
- Evaluation of measurement data in Matlab.

Introduction

Radar sensors are used in many modern cars nowadays. Improving road safety is one of the main concerns in the automotive industry. Trends in automotive development are pushing radar system technology to higher level of demand in automotive applications. The application range reaches from collision prevention assistance for advanced driving assistance systems subsequently autonomous driving to simple parking sensors.

Radar sensors measure information, such as range, azimuth angle and velocity of objects that are in front and within the field of view of the sensor to determine the driving situation. These measurements are used to provide the driving assistance systems with useful information to warn the driver or to take over control of the vehicle to avoid dangerous situations. Environmental conditions such as bad weather or no light should not limit the safety functionality of such systems.

2.1 FMCW Principle of Operation

For the FMCW method, the instantaneous frequency of an RF carrier frequency is linearly changed for a duration of several ms, which corresponds to a frequency change of several hundred MHz (Figure 2.3). The transmitted signal is reflected at a different object. Due to the signal propagation time, the received signal is delayed, so, the observed frequency at a given time is lower in the rising ramp. The frequency difference is a direct measure of the distance to the vehicle. If, however, there is also a relative speed between the two vehicles, the beat frequency is additionally increased due to the Doppler effect. For the determined beat frequency, a linear combination of possible distances and speed values can be found. In order to resolve this ambiguity,

a falling ramp is additionally used, in which case the received frequency is increased by both components, the signal propagation time and the Doppler effect. This results in two different beat frequencies for the rising and for the falling ramp. The addition of these two beat frequencies results in the distance information, the subtraction provides the relative speed between the two vehicles

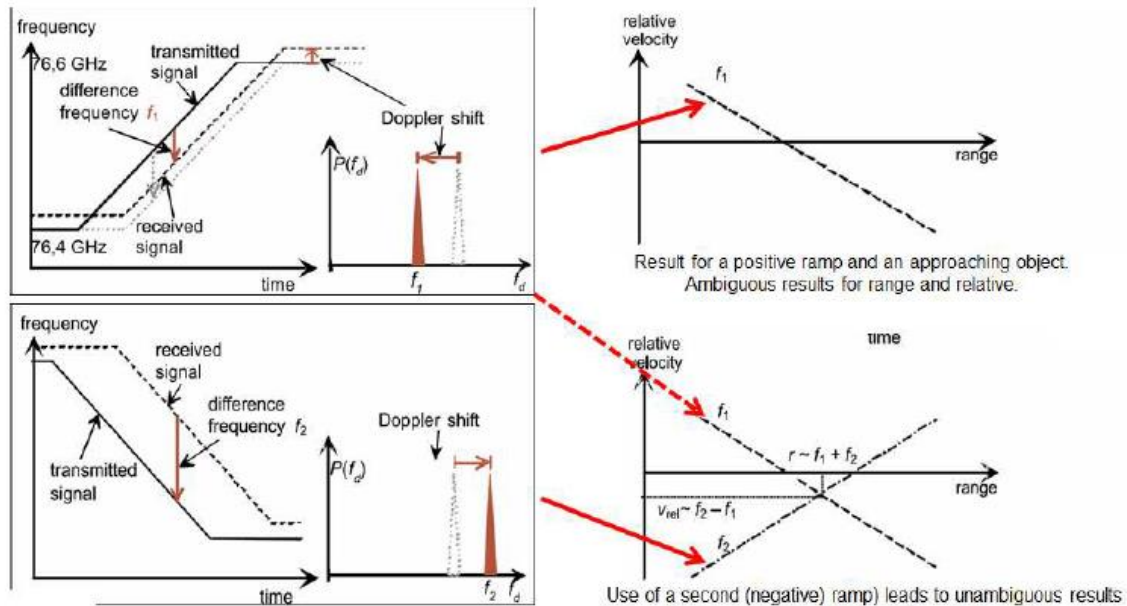


Figure 2.3: FMCW radar working principle. Above, left: positive ramp with an approaching object in time and frequency representation. Above, right: for a measured frequency, only a linear combination of distance and relative speed can be specified due to the ambiguity. Below:

FMCW with a negative ramp for an approaching object. The ambiguity can be resolved by using a second (negative) ramp. [9].

Multiple ramps with different slopes are evaluated for resolving multi-target situations (e.g., traffic situations with several vehicles) [9]. For the analysis of FMCW signals, a method based on a 2D-FFT is often used. The required steps and an exemplary detection result are illustrated in Figure 2.4.

2.2 Description of the Lab Demonstrator

The laboratory demonstrator was designed in the summer term 2014 as part of a study work [2] based on the concept of [3]. Figure 2.5 shows a block diagram of the implemented system. The USB oscilloscope Analog Discovery from Digilent is used to generate the control signal for the VCO (ramp signal) and to read the measured

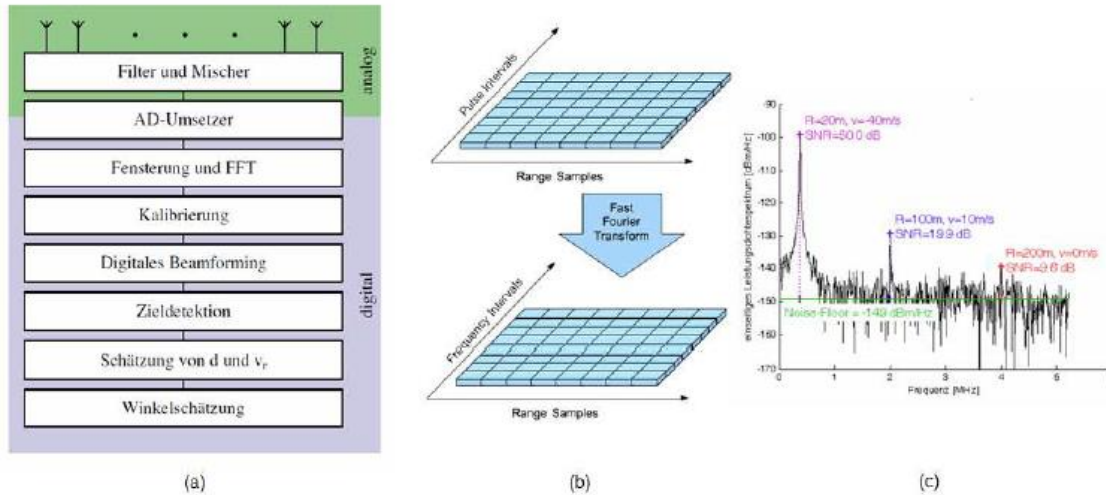


Figure 2.4: Range-Doppler detection using a 2D-FFT approach [10, 8].

data. This module can be accessed directly from Matlab. The maximum sampling rate is 300 kHz.

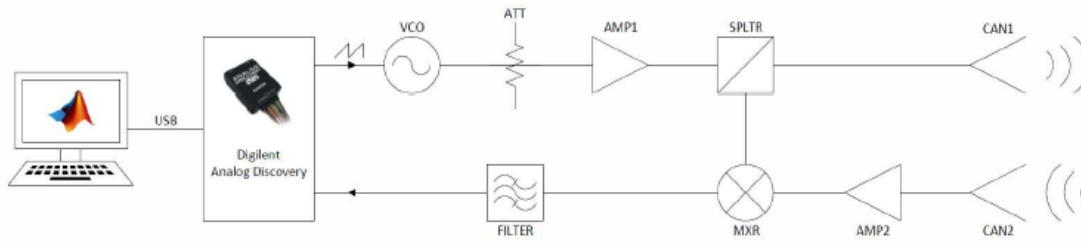


Figure 2.5: Block diagram of the demonstrator [2]. The high-frequency signal path was built with components of the company Mini Circuits, the control of the hardware as well as the reading of the measured data is done via a USB oscilloscope and Matlab.

Table 2.6 provides an overview of the used components. All modules are matched to a 50 impedance and can be connected directly to coaxial connections via SMA adapters. The modules are powered by a 5 V power supply. The most important parameters of the modules are summarized below:

- Voltage Controlled Oscillator (VCO): is used to generate signals in the frequency range from 2315 MHz to 2536 MHz with an output power of 6 dBm.
- Attenuator (ATT): reduces the input power of 6 dBm by about 3.2 dBm at 2.4 GHz. This is a protective measure to avoid overdriving the amplifier.
- Amplifier (AMP1): has a gain of 14 dB. The output power in the 1 dB Compression Point is 18.5 dBm.

- Splitter (SPLTR): relays the input signal to two output channels with an attenuation of 3.26 dB. The transmitter power of the demonstrator is therefore 13.54 dBm or 22.4 mW at 50.
- Frequency Mixer (MXR): mixes the transmitted signal with the received signal.

Further information on the modules can be found in the datasheet section.

Bezeichnung	Beschreibung	Herstellerbezeichnung
VCO	Spannungsgesteuerter Oszillator	ZX95-2536C+
ATT	Dämpfungsglied (3 dB)	VAT-3+
AMP1 / AMP2	Verstärker (14 dB)	ZX60-272LN+
SPLTR	Splitter	ZX10-2-42+
MXR	Frequenzmischer	ZX05-43MH+
	SMA-M auf SMA-M Adapter	SM-SM50+

Figure 2.6: Components and modules for the implementation of the high-frequency signal path [2].

2.3.1 FMCW Radar and startup of the Demonstrator

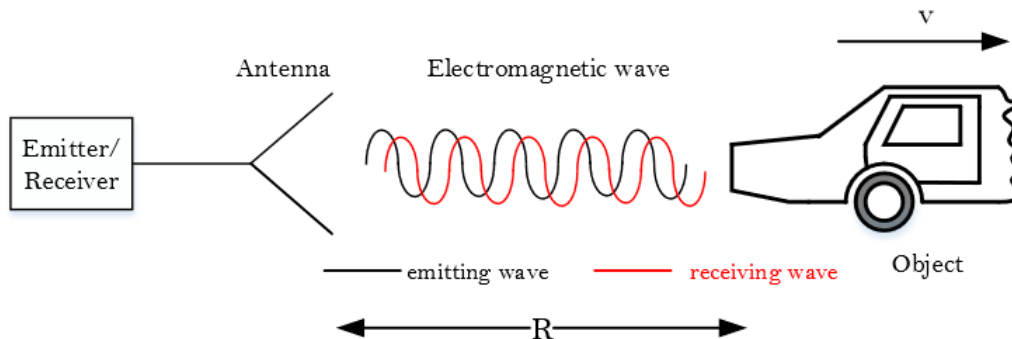


Figure 1

1. The Doppler effect causes the echo/received signal to have a different frequency. The shift of the frequency depends on the relative velocity between the target and the receiver. To derive the Doppler effect, a scenario as depicted in figure is considered. For a distance R between the antenna and the target, the wave is covering N .

$$N = \frac{2r}{\lambda}.$$

The Doppler frequency shift for active radar is as follows, where is Doppler frequency, is transmit frequency, is radial velocity, and is the speed of light.

$$F_D = 2 \times F_T \times \left(\frac{Vr}{c}\right)$$

$$\rightarrow Vr = \left(\frac{F_d \times c}{2 \times F_t}\right)$$

$$\rightarrow Vr = \left(\frac{F_d \times \lambda}{2}\right)$$

where F_D is Doppler frequency, F_T is transmit frequency, Vr is radial velocity, and "C" is the speed of light.

2. The linear FMCW radar modulates the instantaneous frequency by means of a sawtooth signal. The frequency information is used to determine the distance and relative velocity. This can be achieved by using different slope rates. The FMCW signal in figure 2(a) shows a rising slope. Figure 2(b) illustrates a (v/s)-plot, it shows the possible range/velocity combinations for a fixed frequency.

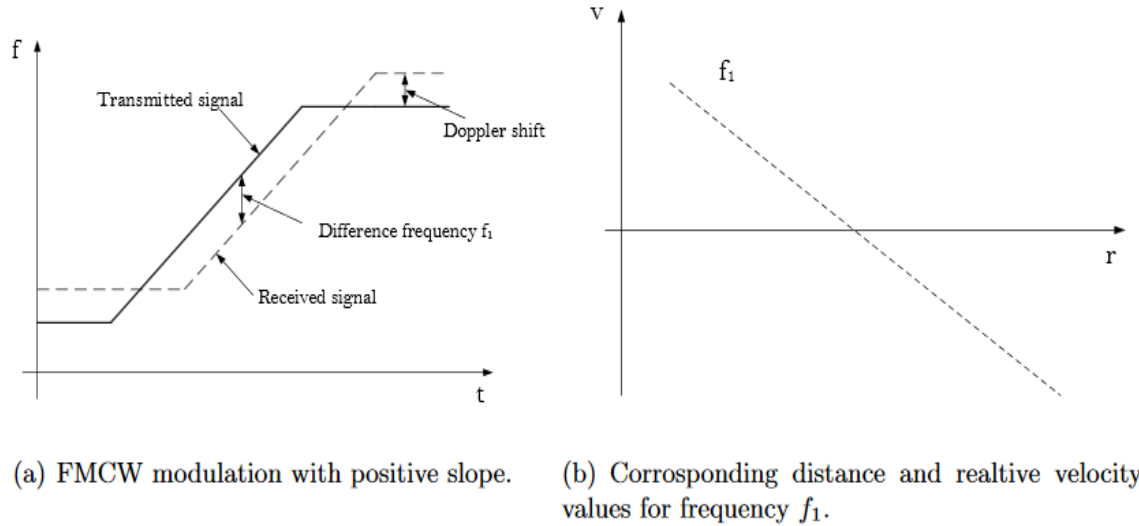


Figure 2

From Figure 2

$$\frac{t_d}{T_s} = \frac{f_b}{B_{Sweep}}$$

$$t_d = \frac{2R}{c}$$

Substituting t_d in Range equation it gives rise to,

$$R = \frac{cT_s f_b}{2B_{\text{Sweep}}}$$

where,

cVelocity of the carrier wave

T_s ...Total Sweep time

f_b ...Band Sweep

The difference frequency will increase when the distance between transmitting and receiving signal rises. This means, the object is moving away from the sensor. Figure 3(a) illustrates the increasing difference frequency for a falling slope when the object is approaching the radar sensor. The linear combination of distance and relative velocity of both frequencies is combined in one (v/s) plot shown in figure 4. The intersection between both slopes gives the relative velocity and distance.

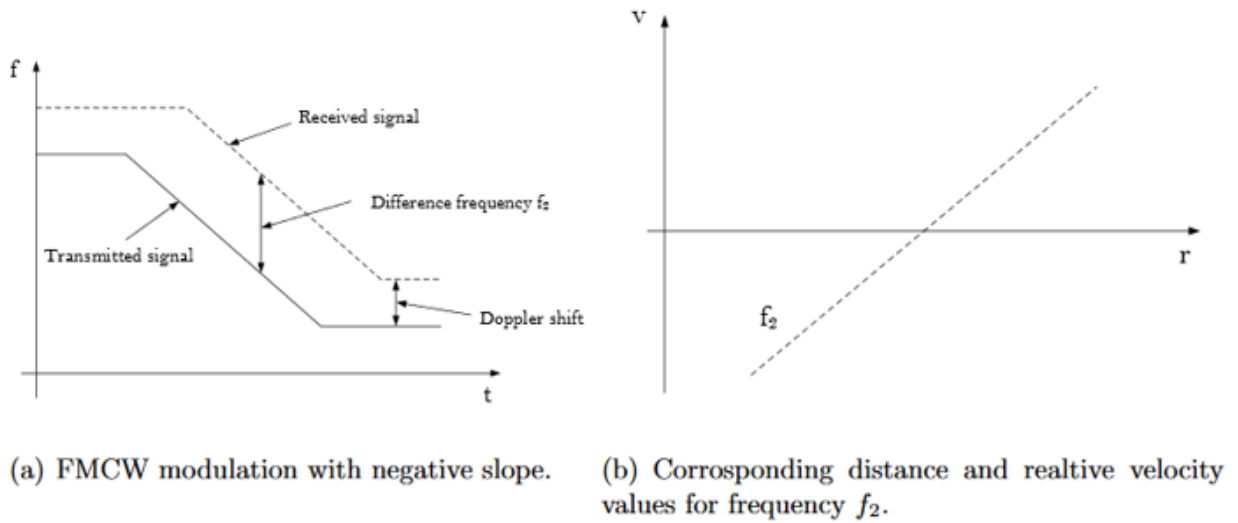


Figure 3

FMCW with several frequency slopes is simple to handle, when detecting only one object. More objects can cause detection problems, because the object frequencies cannot be clearly assigned in the (v/s) plot as shown in figure 5. The first two slopes (solid lines) create for two objects four intersection points, where only two are correct (solid circle). To distinguish between several objects more slopes (dashed lines) can be used to identify the correct objects. The intersection point for all four slopes is only valid for two possibilities (solid circle).

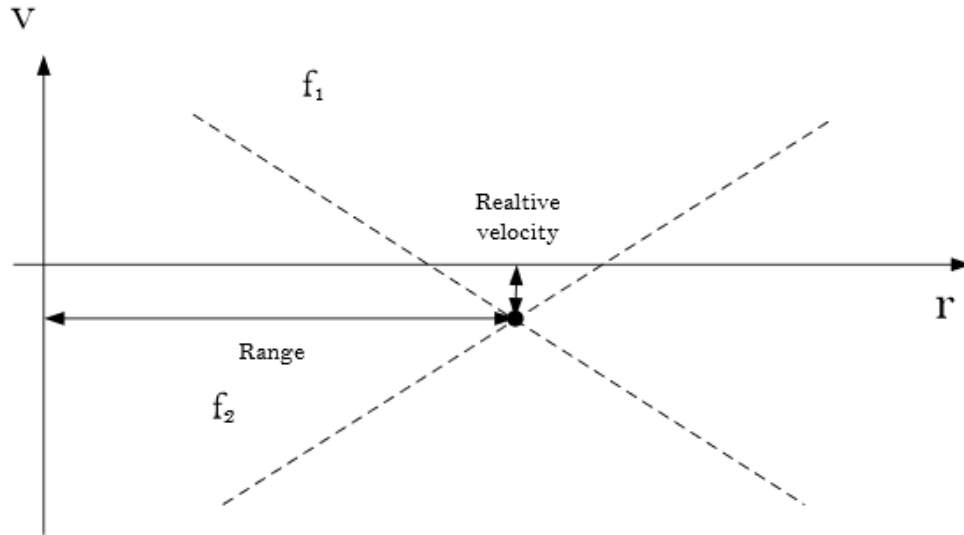


Figure 4

The frequency components f_{bu} and f_{bd} contains the superimposed frequencies of Beat frequency f_b and Doppler frequency f_d for the both positive as well as negative ramps.

$$f_b = \frac{B_{Sweep}}{T_s} \cdot \frac{2R}{c}$$

$$f_d = \frac{2V_r}{\lambda}$$

Applying superposition for the positive and negative ramps:

$$f_{bu} = f_b - f_d$$

$$f_{bd} = f_b + f_d$$

The range and linear velocity could be obtained as:

$$R = \frac{cT_s}{4B_{Sweep}}(f_{bd} + f_{bu})$$

$$v_r = \frac{\lambda}{4}(f_{bd} - f_{bu})$$

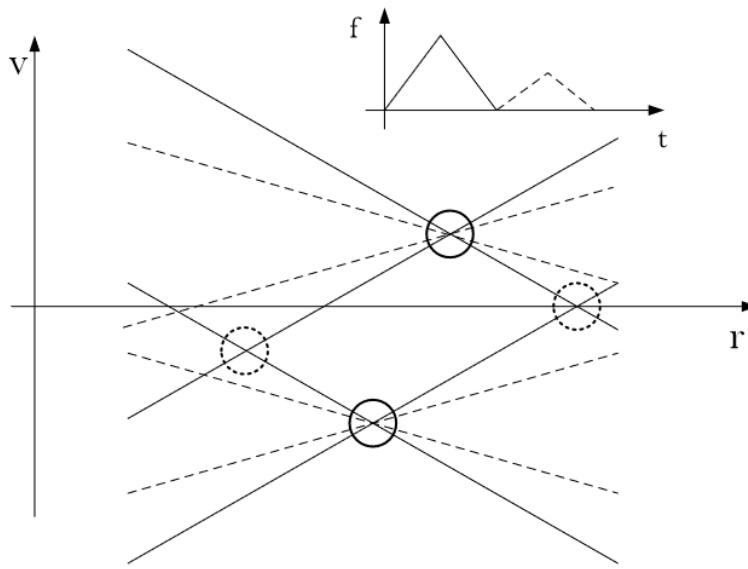


Figure 5

2.3.2 Determination of the length of wire and its influencing parameters.

$$\frac{du}{dt} = \frac{U_{max} - U_{min}}{0.02} = 62.5 \text{ (V/s)}$$

$$\frac{df}{du} = \frac{(2498.1 - 2408.5) \text{ MHz}}{1.25} = 71.68 \text{ MHz/v}$$

The rate of change of frequency is:

$$\begin{aligned} \frac{df}{dt} &= \frac{du}{dt} \times \frac{df}{du} = 62.5 \times 71.68 \times 10^6 \\ &= 4480 \text{ MHz/s.} \end{aligned}$$

[change in freq/m]

$$\frac{df}{ds} = \frac{df}{dt} \times \frac{1}{2.07 \times 10^8}$$

(Note : As per the datasheet, the allowable relative permittivity of the medium is 0.69 times the velocity of the light c.)

$$\frac{df}{ds} = \frac{4480 \times 10^6}{2.07 \times 10^8} = 21.64 \text{ Hz/m}$$

$$1\text{m} \rightarrow 21.64 \text{ Hz/m}$$

$$? \rightarrow 250 \text{ Hz}$$

$$\text{Distance(length)} = 11.55 \text{ m}$$